Reduction Enhancement Mechanisms of a Low-Grade Iron Ore–Coal Composite by NaCl

ZHUCHENG HUANG, RONGHAI ZHONG, LINGYUN YI, TAO JIANG, LIANGMING WEN, and ZHIKAI LIANG

The reduction behavior of a low iron grade with high SiO_2 content ore–coal composite was investigated in the temperature range of 1143 K to 1263 K (870 °C to 990 °C). Sodium chloride was chosen as an additive to promote this reduction process. The effect of the sodium chloride addition and its mechanism was also investigated. Results showed that the added sodium chloride could enhance the reduction of wustite to iron due to the decrease of fayalite, and a higher metallization ratio of reduced sample was obtained. Thermogravimetric–differential scanning calorimeter analysis showed that sodium chloride could greatly facilitate the gasification process of coal and, thus, provide sufficient carbon monoxide to the reduction process of iron oxides. Meanwhile, sodium chloride promoted the reduction process of iron ore pellets directly as the coal gasification effect was excluded. Microstructures of reduced sample revealed that sodium chloride broke the structure of ore and enhanced the growth of newly formed iron particles. As the ore–coal composite with mol (C/Fe = 1.4) and 3 mass pct sodium chloride addition was roasted at 1233 K (960 °C) for 55 minutes, a reduced sample with metallization ration of 74.45 pct could be obtained.

DOI: 10.1007/s11663-017-1116-4

I. INTRODUCTION

THE low iron grade (TFe ~ 33 wt pct)–high silicon dioxide content (SiO_2 ~ 40 wt pct) hematite ore resource with fine particles (average size < 0.045 mm) associated with silicate minerals is difficult to beneficiate by traditional methods.[1,2] However, the total reserve of such iron ore in China (Shanxi province, Hunan province, and Hubei province) is up to 30 million tons. Huge iron ore reserves with similar mineralogy are also found in India and Sudan.[3–5] Effective use of this resource may bring significant benefits to the ironmaking industry in these countries.

Ahmed *et al.*[4] attempted upgrading an iron ore sample containing 36 wt pct TFe and 48 wt pct silica using two-stage separation with a feed size of 0.15 mm. A concentrate containing 64 wt pct TFe at a recovery of 72 pct was obtained. A combined beneficiation process, including stage grinding, low intensity magnetic separation, high intensity magnetic separation, and anionic reverse flotation, was widely adopted to deal with such iron ore in China.[6] Final iron concentrate (TFe 66.95 wt pct, SiO_2 2.95 wt pct) with iron recovery of 72.62 wt pct could be obtained as raw ore was ground to <0.045 mm accounting for 93.81 pct. However, its long process flow with extremely high cost and energy consumption still exists. The coal-based direct reduction followed by magnetic separation has been found to be another effective way and has been actively researched.[2,7,8] The raw ore (TFe 43.18 to 47.66 wt pct, SiO_2 17.1 wt pct) was reduced at 1473 K (1200 °C) for 40 to 60 minutes to obtain reduced samples with metallization degree 95 pct.[9,10] A typical low iron grade (with TFe 27 wt pct, SiO_2 49.51 wt pct, and iron oxide particle size <0.005 mm) was reduced at 1423 K (1150 °C) for 100 minutes, and reduced products with 94 pct metallization degree were obtained.[2] Concentrates with grades of 85 to 95 pct were achieved by milling-magnetic separation, and iron recovery was higher than 80 pct. However, for the high SiO_2 characteristic, low melting point phase, such as fayalite (Fe_2SiO_4), formation occurs (Table I).[11,12] This fayalite hindered further reduction process of iron oxide.[13,14] Fayalite melts around 1400 K (1200 °C) into liquid, which leads to ring formation in the rotary kiln or rotary hearth furnace, thus disrupting normal operations. Therefore, promoting FeO reduction to metallic iron and minimizing fayalite formation is of great concern in an optimized reduction process for this SiO_2-rich ore.

The reduction of iron ore–coal composite pellets has been an important subject in the area of coal-based

ZHUCHENG HUANG, RONGHAI ZHONG, LINGYUN YI, TAO JIANG, LIANGMING WEN, and ZHIKAI LIANG are with the School of Minerals Processing & Bioengineering, Central South University, Changsha 410083, Hunan, China. Contact e-mail: ylycsu@126.com

Manuscript submitted April 10, 2017.
Article published online November 1, 2017.

Table I. Melt Point of Different Compound Systems Formed by Fe_2SiO_4

System	Liquid Characteristics	Melt Temperature
SiO_2-FeO	Fe_2SiO_4	1478 K (1205 °C)
	Fe_2SiO_4-SiO_2	1451 K (1178 °C)
	Fe_2SiO_4-FeO	1451 K (1178 °C)
Fe_3O_4-Fe_2SiO_4	Fe_2SiO_4-Fe_3O_4	1415 K (1142 °C)

Table II. Main Chemical Composition of the Ore (Weight Percent)

TFe	SiO_2	Al_2O_3	CaO	MgO	MnO	P	S
33.86	40.61	4.36	1.57	1.05	0.04	0.38	0.082

reduction research.[15–18] CO generated within the iron ore–coal composite pellets reacts with iron oxides. Moreover, the Boudouard reaction increased the inner pressure of composite and, therefore, accelerated the diffusion process. Apart from these two points, the direct contact between the iron oxides and coal also enhanced the dynamics condition of reduction for shorting the diffusion distance of CO and the availability of a large number of reaction sites.[18,19] Besides, it was reported that suitable additives could effectively facilitate the reduction of iron oxide.[20,21] As a widely used one, alkali metal salt, such as Na_2CO_3, Na_2SO_4, and CaF_2, could promote the gasification reaction of carbon.[22–24] Lattice distortion and structure defects in mineral caused by alkali metal salt were supposed to be another reason for their facilitating effect on the overall reduction process.[25,26] However, varieties of salts always produced different responses.

In this article, iron ore–coal composite pellet reduction technology was proposed to use a typical low iron grade but high SiO_2 content iron ore, and optimized reduction conditions were advised. Compared with previous works, a lower temperature was adopted. Otherwise, in order to minimize fayalite-type phase formation and enhance iron oxide reduction, NaCl was chosen as an additive in our ore–coal composite. The effect of NaCl on reduction behavior and its mechanism was investigated by applying a thermogravimetric–differential scanning calorimeter (TG-DSC), X-ray diffraction (XRD), and scanning electron microscope–energy dispersive spectroscope (SEM-EDS).

II. EXPERIMENTAL

A. *Materials*

A typical low iron grade but high SiO_2 content iron ore from Hunan province in China was raw material for this research. As shown in Table II, the total iron content in the iron ore was 33.86 wt pct, while the content of SiO_2 was 40.61 wt pct. Other constituents included 4.36 wt pct Al_2O_3.[1,3] 1.57 wt pct CaO, and 1.05 wt pct MgO. The XRD pattern in Figure 1 reveals that mineral phases in the ore were mainly hematite, quartz, chlorite, and sericite.

The microstructural images of the ore are presented in Figure 2. The majority of hematite grains presented extremely complex embedded characters with gangue substrate. Therefore, it was difficult to obtain the ideal separation index by traditional beneficiation process, e.g., flotation or magnetic separation. In our research, the ore was crushed (PE60 × 100-mm crusher, Zhengzhou YiJu Poly Machinery Equipment Co., Ltd., Henan, China) to – 1 mm and then milled (ZQM-150 × 50 mm) into powders (– 0.045 mm, accounting for 69.20 pct) for the pelletizing procedure.

Reductant coal used in this research was a bituminous, produced in Shanxi province, China. Proximate analysis of the coal is shown in Table III. The coal was crushed (JC56 jaw crusher, Zhengzhou YiJu Poly Machinery Equipment Co., Ltd., Henan, China) to – 1 mm and then milled (ZQM-150 × 50 mm, Zhengzhou YiJu Poly Machinery Equipment Co., Ltd.) into powders (–0.045 mm accounting for 58.89 pct) for pelletizing procedure. The additive NaCl used was analytical reagent, with a purity > 99.56 pct (Changsha Chemical Reagent Co., Ltd., Changsha, China).

B. *Methods*

First, raw ore, coal (mole ratio of C/Fe was 1.4), a certain amount of NaCl, and 1 pct of bentonite (used as a binder) were mixed to produce pellets. Then the mixture was pelletized into composite pellets at an average size of 5 mm in a disc pelletizer (diameter = 1000 mm, rim height = 300 mm, angle of inclination = 45 deg, and rotational speed = 28 rpm). Also, the green composite pellets were dried at 383 K (110 °C) for 3 hours. For comparison, pellets without coal were prepared in the same way for the following reduction procedure.

The reduction experiments of composite pellets were carried out in a horizontal tube furnace (HTF-1, Changchen Electric Furnace Co. Ltd., Changsha, China), as shown as Figure 3. The furnace temperature was controlled by a digital temperature controller (accuracy ±1 °C). The target temperature of the heating zone was measured by a Pt-Rh thermocouple located in the center of the furnace. After the furnace was preheated to the desired temperature, nitrogen was inlet (at a rate of 100 mL/s) to drive the air out of the quartz tube. Composite pellets (10 ± 0.01 g) were placed in an alumina porcelain boat (80 mm × 10 mm) and pushed into the heating zone. After that, the nitrogen flow rate

was turned down to 50 mL/s[27] [standard temperature and pressure (STP) condition] immediately. At the end of the required reduction time, pellets were quickly taken out and quenched by liquid nitrogen. Pellets without coal were reduced by CO in the same apparatus. When the alumina porcelain boat was pushed into the heating zone, nitrogen was shifted to CO immediately. Other steps were the same as the reduction experiments of composite pellets. The purity of gases (CO and N_2) used in the tests was higher than 99.99 vol pct (Changsha Gas Making Co., Ltd., Changsha, China). Each experiment was tested four times and the average value was calculated.

The phase constituents of the reduction samples were identified by copper K_α X-ray source XRD (D/max 2550PC, Rigaku Co., Ltd., Tokyo, Japan) with the step of 0.02 deg at 10 deg min^{-1} ranging from 10 to 80 deg. Also, a voltage of 40 kV and a current of 250 mA were used. Morphological analysis and microzone chemical composition of the samples were analyzed with an SEM-EDS (JSM-6510A, Japan Electron Optics Ltd., Tokyo, Japan). Also, the acceleration voltage of the

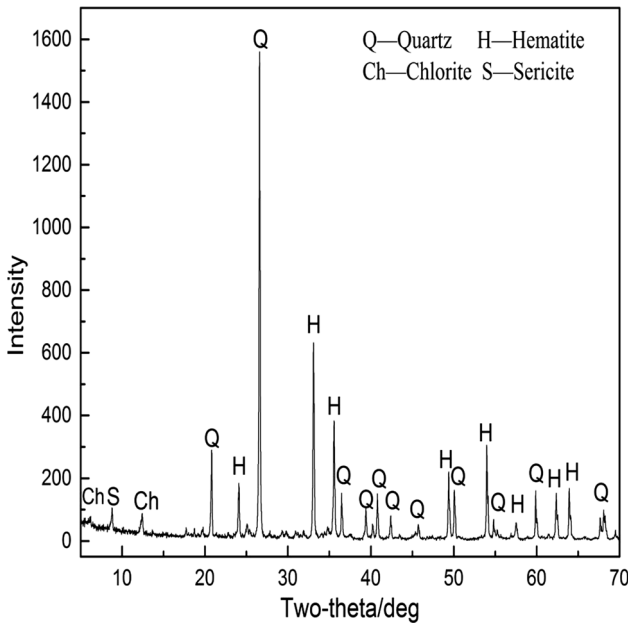

Fig. 1—X-ray diffraction pattern of the iron ore.

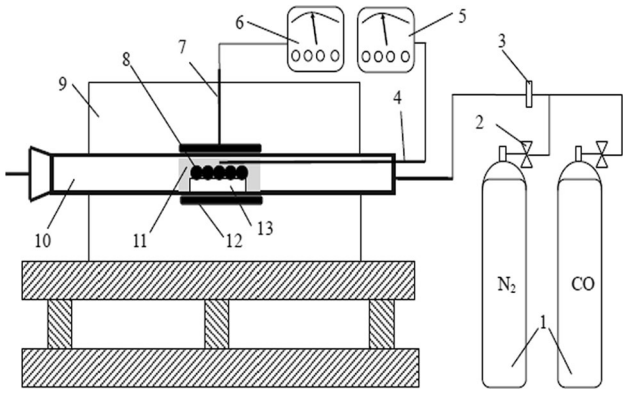

Fig. 3—Schematic diagram of the experimental apparatus for the reduction process: 1—gas cylinder, 2—pressure regulator, 3—flowmeter, 4—Pt-Rh thermocouple, 5—heating zone temperature indicator, 6—digital temperature controller, 7—thermocouple, 8—samples, 9—furnace, 10—quartz tube, 11—uniform temperature zone, 12—heating resistor, and 13—alumina porcelain boat.

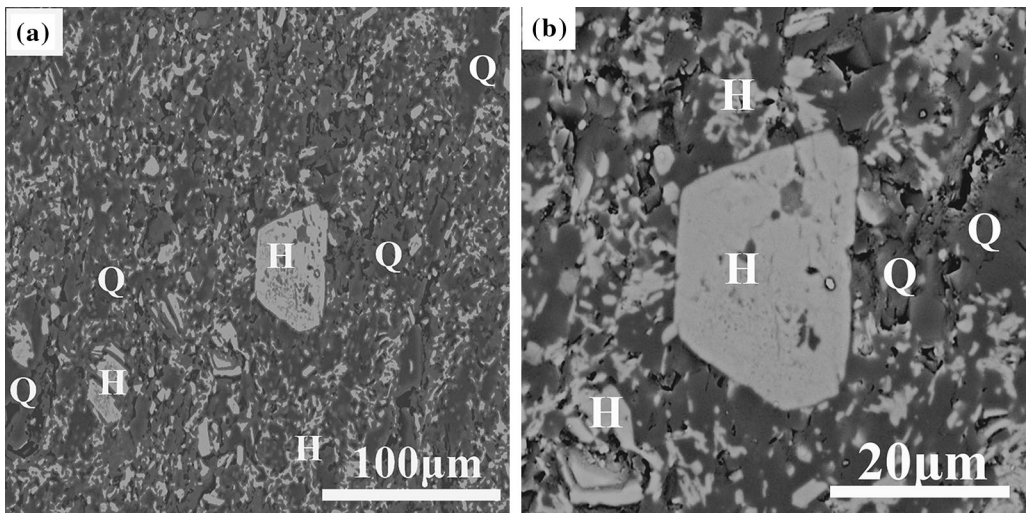

Fig. 2—SEM image of the iron ore: (*a*) micrograph of iron ore with magnification 2000 times and (*b*) micrograph of iron ore with magnification 5000 times. H—hematite (white particles), Q—quartz (black particles).

Table III. Proximate Analysis of the Coal (Weight Percent)

Fixed Carbon	Moisture	Ash	Volatile Matters
58.53	5.16	15.44	20.87

SEM was 30 kV. TG-DSC analysis of coal under CO_2 was performed using a thermogravimetric analyzer (STA-449C, Netzsch Co., Ltd., Germany). To ensure mixture uniformity of NaCl and coal powder, NaCl was dissolved by distilled water and then mixed with coal. The mixture was dried at 383 K (110 °C) for 3 hours. For TG-DSC tests, 0.05 g (±0.0001 g) dried mixture was used. Experiments were carried out under nonisothermal temperature, from room temperature 298 K to 1273 K (25 °C to 1000 °C) with a heating rate of 10 °C/min. The flow rate of CO_2 was 20 mL/s.

The degree of metallization of reduction products (η_{Fe}) was calculated by the following formula:

$$\eta_{Fe} = (MFe/TFe) \times 100 \text{ pct}, \quad [1]$$

where TFe was the total Fe in reduction products and MFe was the metallic Fe content in the reduction products. Both MFe and TFe were analyzed by chemical analysis four times, and average values were calculated. The content of fayalite was further calculated according to XRD data.

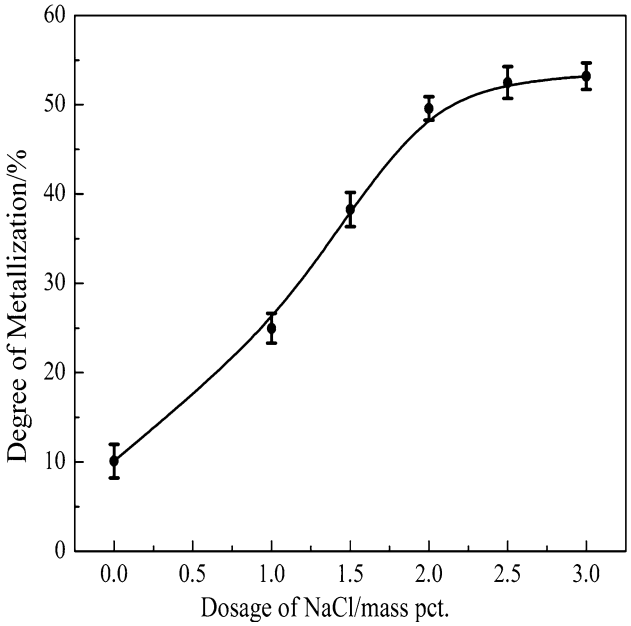

Fig. 4—Effects of NaCl on the degree of metallization of reduced composite pellets.

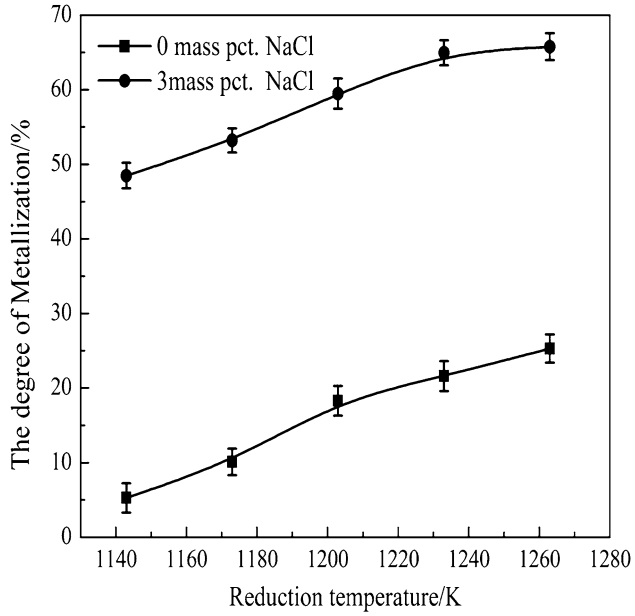

Fig. 6—Effect of temperature on the degree of metallization of reduced composite pellets.

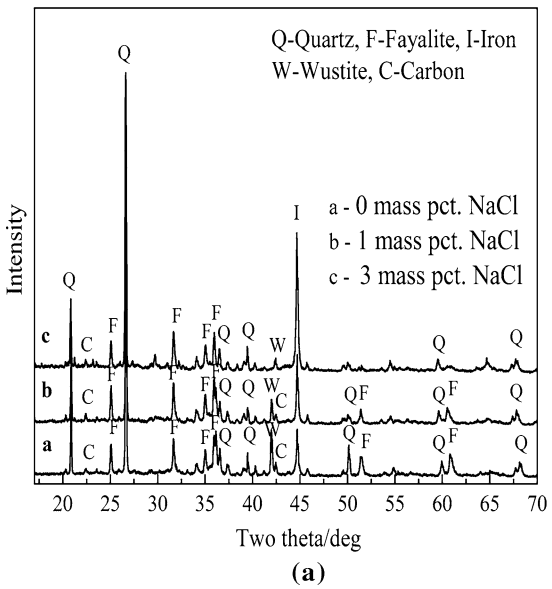

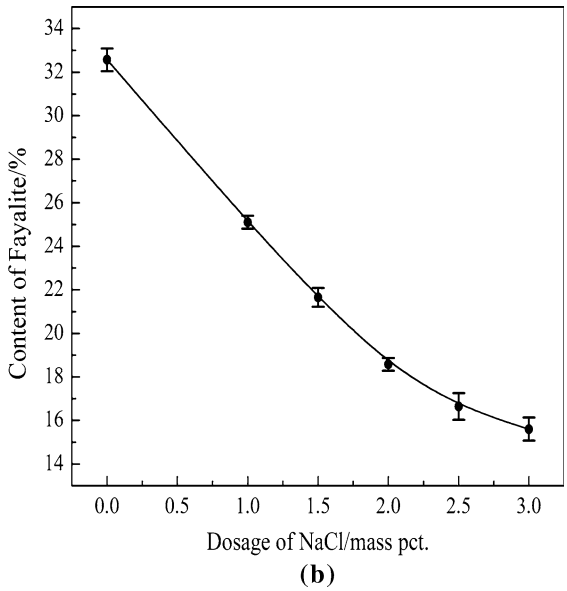

Fig. 5—X-ray diffraction analysis of reduced composite pellets (reduced at 1173 K (900 °C) for 35 min) with different dosages of NaCl: (*a*) XRD pattern of pellets with 0, 1, and 3 mass pct NaCl. (*b*) Effects of NaCl on content of fayalite in reduced pellets.

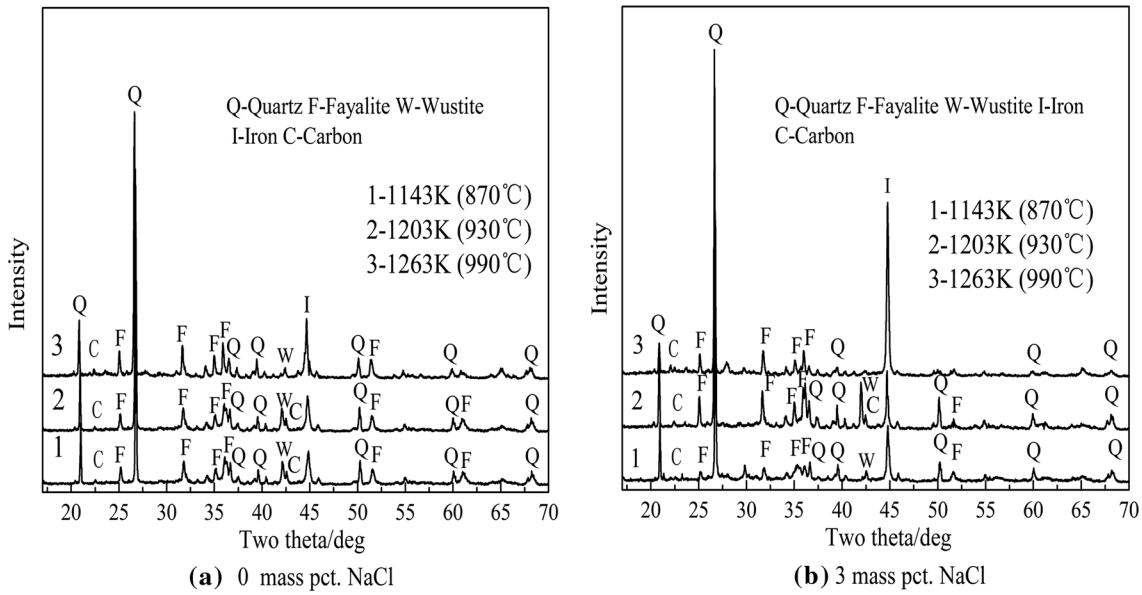

Fig. 7—X-ray diffraction pattern comparison of roasted pellets reduced at different temperatures. (*a*) XRD of pellets with 0 mass pct NaCl, reduced at 1143 K, 1203 K, and 1263 K (870 °C, 930 °C and 990 °C). (*b*) XRD of pellets with 3 mass pct NaCl, reduced at 1143 K, 1203 K, and 1263 K (870 °C, 930 °C and 990 °C).

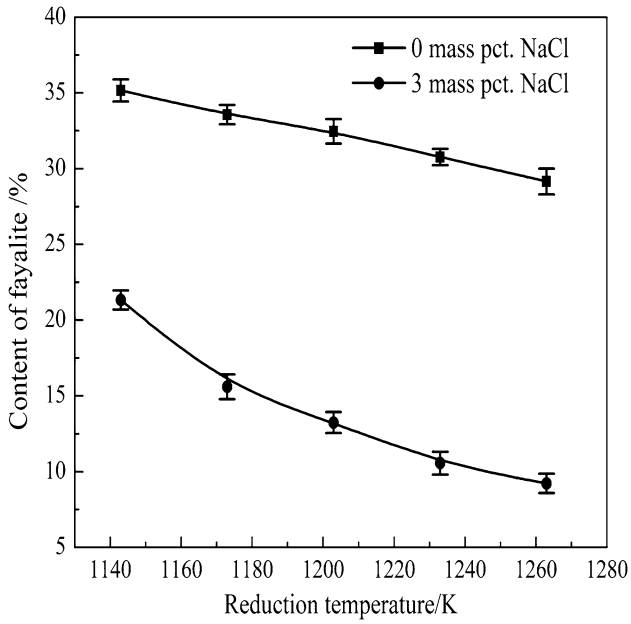

Fig. 8—Effect of reduction temperature on content of fayalite.

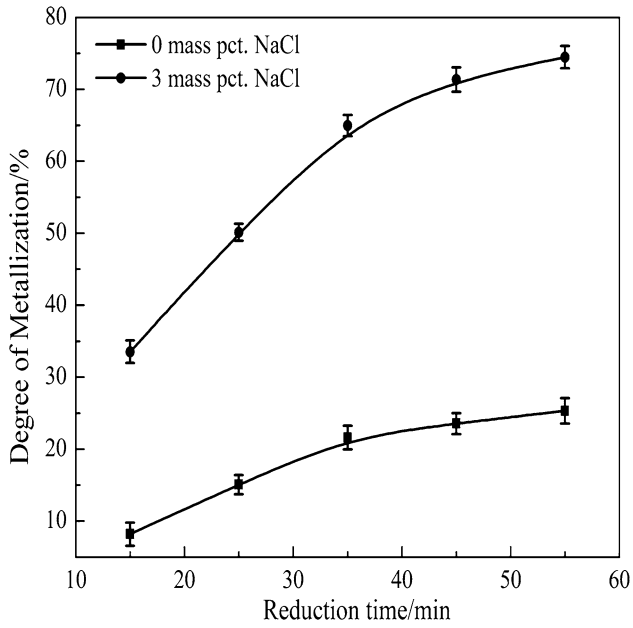

Fig. 9—Effect of additives on the metallization degree of composite pellets within different reduction times, 1223 K (960 °C).

III. RESULTS AND DISCUSSION

A. *Reduction Behavior of Composite Pellets*

1. *Effect of NaCl additions on the reduction of composite pellets*

The effect of NaCl on the degree of metallization of reduced composite pellets is shown in Figure 4. It can be observed that the degree of metallization of reduced pellets increased sharply when a certain amount of NaCl was added. When reduced at 1173 K (900 °C) for 35 minutes, the degree of metallization of pellets without NaCl was extremely low, 10.09 pct only. With 1, 2 mass pct NaCl added, the degree of metallization increased to 24.96 and 49.57 pct, respectively. However, above 2 mass pct additions, the reduction enhancement of the composite pellets was not pronounced and seemed to plateau. Further, the degree of metallization reached 53.19 pct when 3 mass pct NaCl was added. The results suggest that the reduction process was promoted effectively by NaCl.

Products reduced at 1173 K (900 °C) for 35 minutes were analyzed by XRD. XRD patters and quantitative analyses of fayalite calculated according to XRD data

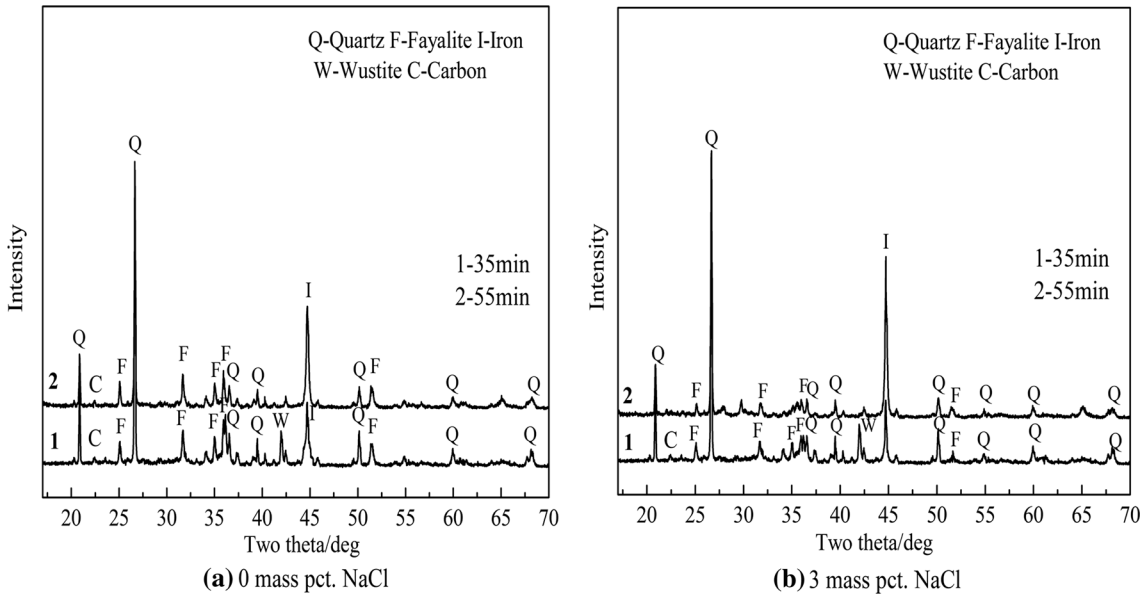

Fig. 10—Comparison of X-ray diffraction patterns of products within different reduction times: (*a*) XRD of pellets with 0 mass pct NaCl, reduced for 35 and 55 min. (*b*) XRD of pellets with 3 mass pct NaCl, reduced for 35 and 55 min.

are shown in Figure 5. Figure 5 shows that the main phases in reduced pellets were quartz (SiO_2), metallic iron (Fe), fayalite (Fe_2SiO_4), and wustite (FeO). The weight of metallic iron was pretty low, and the weight of wustite was high without NaCl, which suggests that pellets were poorly reduced. As 1 mass pct NaCl was added, the weight of metallic iron increased, while those of wustite and fayalite decreased. When 3 mass pct NaCl was used, metallic iron increased obviously, and fayalite and wustite decreased sharply.

Reduction of Fe_2O_3 followed the process of Fe_2O_3, Fe_3O_4, FeO, and Fe. Reduction of Fe_2O_3 to FeO occurred rapidly, while the reduction of FeO to Fe always proceeded laggardly, as wustite needs higher reduction potential for conversion to iron.[28–30] Since the iron ore used in this study contained a large amount of SiO_2 (40.61 pct), reduction intermediate FeO (unstable) could inevitably react with SiO_2 (stable), forming fayalite (stable)[11,12]:

$$\begin{aligned} &\mathrm{FeO} + \mathrm{CO} = \mathrm{Fe} + \mathrm{CO_2} \\ &\Delta G_T^{\theta} = -22,800 + 24.26T\,(\mathrm{J/mol}), \end{aligned} \quad [2]$$

$$\begin{aligned} &2\mathrm{FeO} + \mathrm{SiO_2} = \mathrm{Fe_2SiO_4} \\ &\Delta G_T^{\theta} = -76,415.42 + 33.79T\,(\mathrm{J/mol}). \end{aligned} \quad [3]$$

Once FeO transformed into Fe_2SiO_4, it could hardly be reduced to metallic iron.[13] The XRD analysis of pellets without NaCl shows that, rather than being reduced to metallic iron, a large amount of FeO reacted with SiO_2 and formed Fe_2SiO_4. Besides, a portion of FeO still remained unreduced. Therefore, the degree of metallization was pretty low. Since Reaction [3] was inhibited effectively when 3 mass pct NaCl was added, the reduction of FeO was facilitated largely. The result was in agreement with earlier researchers.[31]

2. *Effect of reduction temperature*

The effect of temperature on the degree of metallization of reduced pellets (reduction time was 35 minutes) is shown in Figure 6.

It can be observed that the degree of metallization of pellets both without NaCl and with 3 mass pct NaCl increased with an increase of temperature, and the latter was much higher than the former. The degree of metallization of pellets without NaCl was 5.26 pct when reduced at 1143 K (870 °C), and that of pellets with 3 mass pct NaCl was 48.47 pct. When reduced at 1263 K (990 °C), the degree of metallization of pellets without NaCl and with 3 pct NaCl was increased to 25.29 and 64.95 pct, respectively. These results suggest that a higher degree of metallization can be obtained at relatively higher temperature.

The products reduced at 1143 K, 1203 K, and 1263 K (870 °C, 930 °C and 990 °C) were further analyzed by XRD. The results are shown in Figure 7, and the contents of fayalite are shown in Figure 8. The weight of metallic iron without NaCl was lower than that with 3 mass pct NaCl. Without NaCl addition (in Figure 7(a)), the weight of fayalite changed slightly as the temperature increased, while metallic iron phase increased with the further reduction of wustite. In the case of 3 mass pct NaCl used (Figure 7(b)), metallic iron phase increased obviously along with the cutback of fayalite, and wustite was found to be negligible as the temperature rose to 1263 K (990 °C).

The reduction reaction of iron oxide was inactive at lower temperatures. Lower temperature also restrained the reactivity of the Boudouard reaction, which led to lower partial pressure or concentration of CO. Thus, the

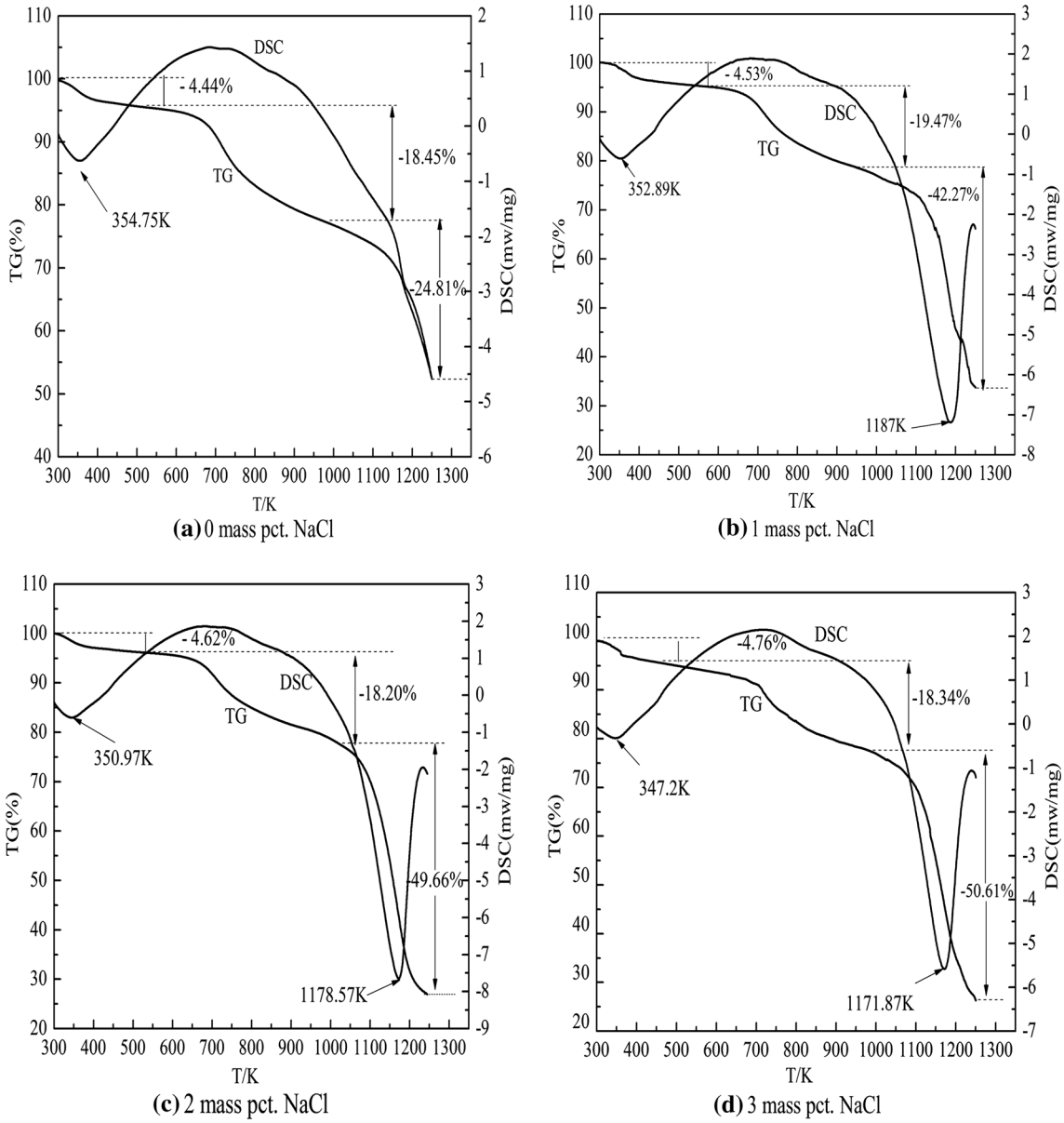

Fig. 11—Effects of NaCl on TG-DSC curves of gasification reaction of coal: (*a*) TG-DSC curves of gasification reaction of coal with 0 mass pct NaCl, (*b*) TG-DSC curves of gasification reaction of coal with 1 mass pct NaCl, (*c*) TG-DSC curves of gasification reaction of coal with 2 mass pct NaCl, and (*d*) TG-DSC curves of gasification reaction of coal with 3 mass pct NaCl.

reduction rate of FeO was further hindered. As a result, the large amount of FeO was reacted with quartz and formed Fe_2SiO_4, rather than being reduced to metallic iron. The reduction rate and gasification were improved at higher temperature, which enhanced reduction of FeO and, thus, decreased the amount of fayalite. According to XRD results, it can be inferred that an increase of the degree of metallization without NaCl as the temperature increased was mainly caused by the further reduction of FeO (Reaction [2]) that had not been reduced at lower temperature, while the contribution of fayalite formation (Reaction [3]) inhibition was tiny. The results suggested that ideal reduction results cannot take place if fayalite formation was not inhibited. With 3 mass pct NaCl addition, contribution of fayalite inhibition was enhanced effectively and the degree of metallization increased obviously.

3. *Effect of roasting time*

Figure 9 reveals that the degree of metallization of reduced pellet increased obviously with prolonged reduction time (reduction temperature was 1233 K (960 °C)). It was easy to understand that reduction proceeded to a greater extent with the prolonged reaction time. However, the increase of metallization degree differed widely between without NaCl and with 3 mass pct NaCl used. The degree of metallization without NaCl reached 25.33 pct as it was reduced for 55 minutes. However, the degree of metallization of 74.45 pct was obtained as 3 mass pct NaCl used. The effect of

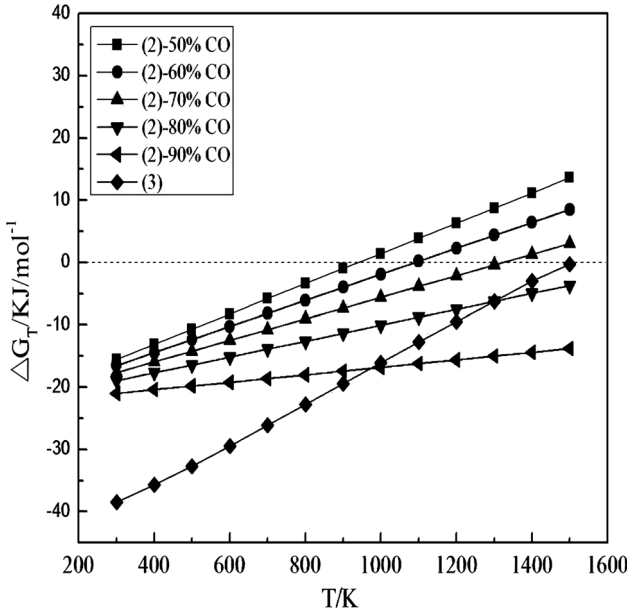

Fig. 12—Effects of CO concentration on Gibbs free energy of Reactions [2] and [3].

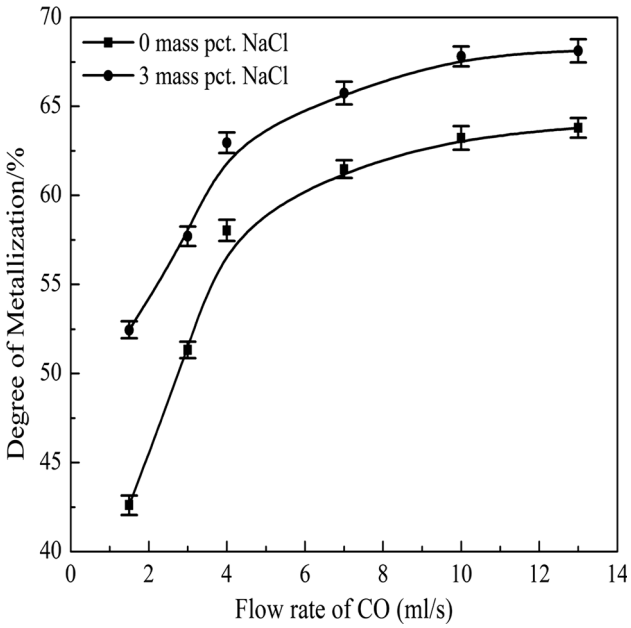

Fig. 13—Effect of flow rate of CO on the degree of metallization of pellets.

reduction time on phase transformation was examined by XRD, as presented in Figure 9.

As presented in Figure 10(a), the iron phase increased along with the decline of wustite as the reduction time was prolonged, but fayalite in pellets showed little variation. It can be inferred that the reduction of wustite to iron was promoted with prolonged time in NaCl-free composite. Figure 10(b) shows that there was a decrease of fayalite phase with 3 mass pct NaCl (compared with NaCl free) besides the reduction of wustite to iron. The inhibition of fayalite and reduction of wustite could

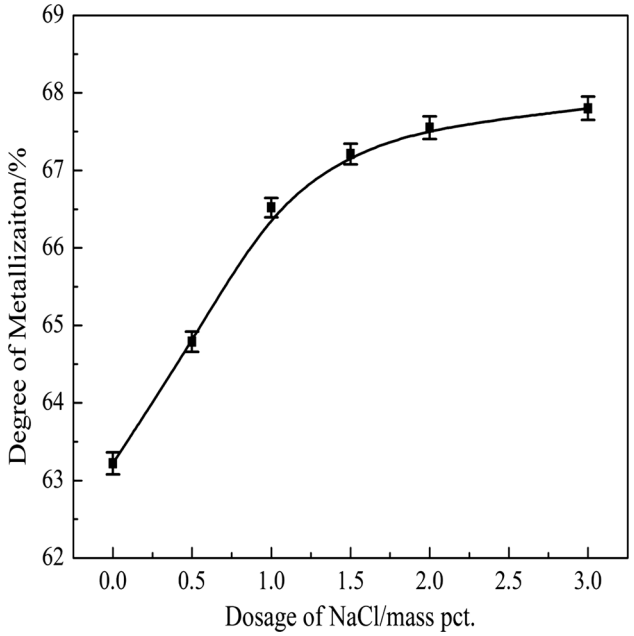

Fig. 14—Effect of NaCl on the degree of metallization of iron ore pellets without NaCl.

both be improved in the NaCl addition composite, which led to a higher degree of metallization of reduced as compared with NaCl-free pellet.

B. *Reduction Enhancement Mechanism of Sodium Addition*

1. *Effect of NaCl on coal gasification*

TG-DSC analyses were carried out to define the effects of NaCl on the coal gasification reaction with CO_2. Reduction reactions of coal-based direct reduction are shown as follows:

$$Fe_xO_y + C = Fe_xO_{y-1} + CO, \quad [4]$$

$$Fe_xO_y + CO = Fe_xO_{y-1} + CO_2, \quad [5]$$

$$CO_2 + C = 2CO \quad \Delta G_T^{\theta} = 170,700 - 174.5T\,(J/mol). \quad [6]$$

For carbothermal reduction, the rate of the indirect reduction Reaction [5] is much faster than the direct reduction Reaction [4] when mass CO is generated. The reduction of iron ore is considered mainly composed of indirect reduction and carbon gasification. Therefore, it is necessary to research the effect of NaCl on gasification of coal with CO_2; the results are shown in Figure 11 (flow rate of CO_2 was 20 mL/s).

As can be seen in Figure 11, weight loss during the interval of 273 K to 473 K (0 °C to 200 °C) was caused by water evaporation, and the weight losses of four samples were nearly the same. Weight loss during 473 K to 973 K (200 °C to 700 °C) was mainly caused by the

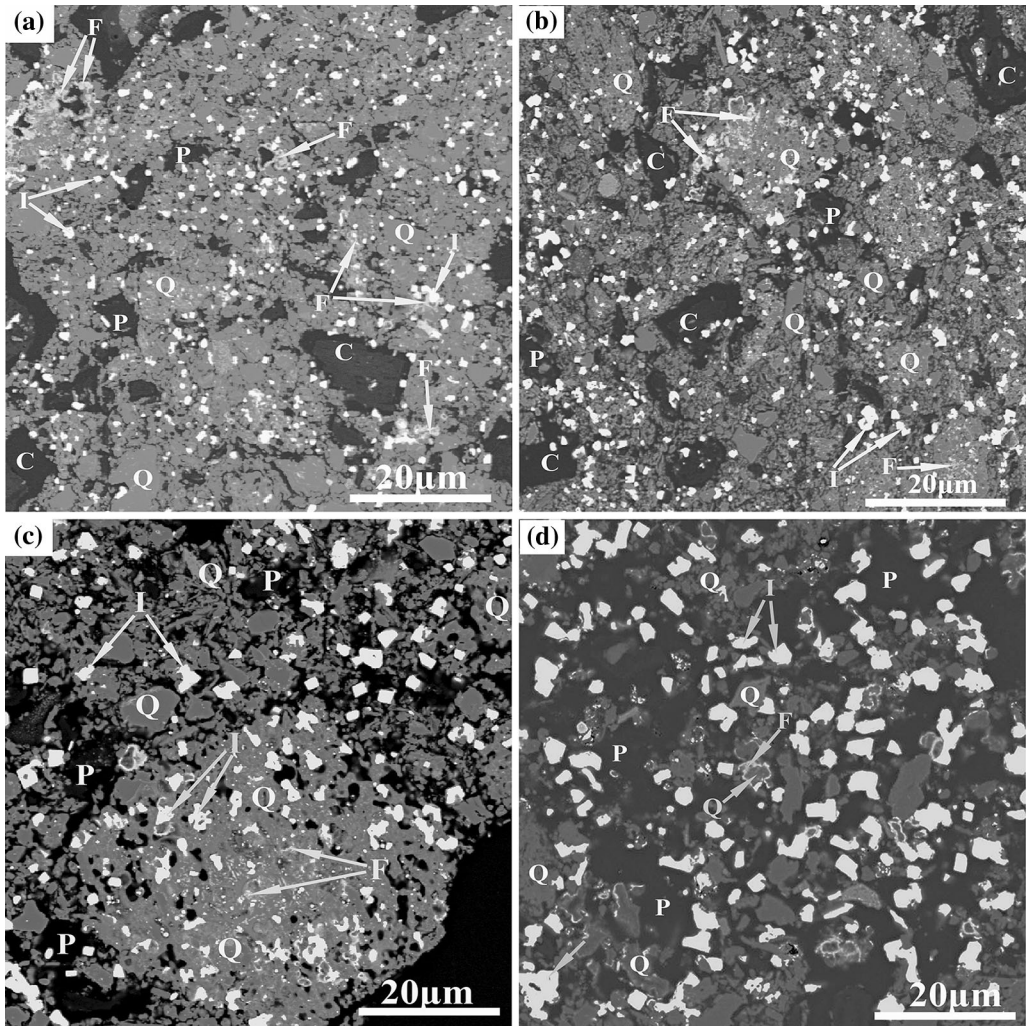

Fig. 15—Microstructure of reduced pellets with different NaCl: (*a*) micrograph of reduced pellet with 0 mass pct NaCl, (*b*) micrograph of reduced pellet with 1 mass pct NaCl, (*c*) micrograph of reduced pellet with 2 mass pct NaCl, and (*d*) micrograph of reduced pellet with 3 mass pct NaCl. I—iron, P—pore, F—fayalite, Q—quartz, and C—carbon.

removal of volatile matters, and weight transformations of samples were similar. When the temperature was above 973 K (700 °C), weight loss was mainly attributed to the gasification reaction of fixed carbon with CO_2 (Reaction [6]).

The TG curves show that above 1173 K (900 °C), weight loss of coal without NaCl was 24.81 pct, far below that of coal with NaCl. This means that the gasification extent was rather low, which led to a low CO/CO2 ratio in the context of reduction in a composite system. It is disadvantage for the reduction of wustite to metallic iron. Hence, the possibility of fayalite formation was increased (Reaction [3]). As 1 mass pct, 2 pct, and 3 mass pct NaCl were added, the weight losses of samples were increased to 42.27, 49.66, and 50.61 pct, respectively. Gasification of coal was facilitated effectively by NaCl; thus, the ratio of CO/CO_2 was increased.[25]

The standard Gibbs free energy (ΔG_T^θ) change of the related reactions was calculated as follows:

$$\Delta G_T^\theta = -RT \ln K^\theta, \qquad [7]$$

where R is the ideal gas constant (8.3144 J/mol K), T is the temperature in Kelvin (K), and K^θ is the standard equilibrium constant. The nonstandard Gibbs free energy (ΔG_T) change of the related reactions (Eq. [2]) was calculated as follows:

$$\Delta G_T = \Delta G_T^\theta + RT \ln P, \qquad [8]$$

where P is the reaction quotient at the given condition.

Suppose that the reaction is carried out at a constant pressure of 1 atm (p^θ) and the CO gases are of a certain partial pressure; then the $\Delta G_T - T$ relationship at various temperatures can be obtained according to Eq. [7]. Subsequently, based on the value of $P = p$' gas/p^θ, the ΔG_T of Eq. [2] was calculated according to Eq. [7]. The $\Delta G_T - T$ changes of Eq. [2] as a function of the partial pressure of CO and comparison with Eq. [3]

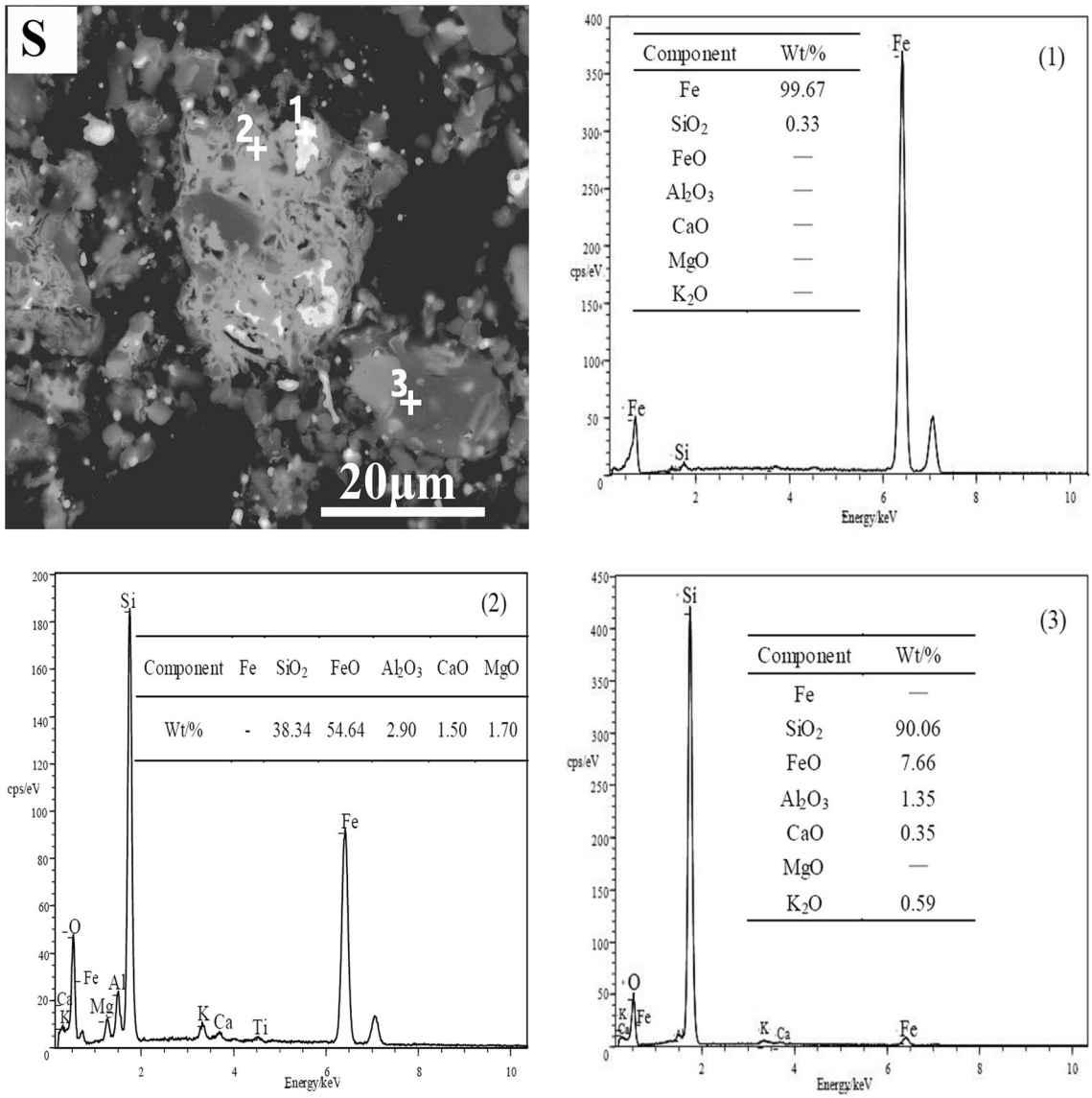

Fig. 16—SEM-EDS analysis of the reduced pellets with no NaCl. S—SEM of reduced pellet. (1), (2), and (3)—EDS analyses of positions 1, 2, and 3.

are plotted in Figure 12. CO concentration affects the reduction of FeO obviously, according to Gibbs free energies. The Gibbs free energies of Reaction [2] were decreased with the increase of CO concentration, which means they take place easier. This is critical during the reduction roasting of the ore and also is anticipated. With NaCl added, the extent of gasification Reaction [6] of coal was promoted sharply; thus, CO concentration was increased effectively. As a result, Reaction [2] was enhanced. Therefore, FeO was mainly reduced to Fe rather than being shifted into Fe_2SiO_4, even if it could not be avoided completely.

The DSC curves of coal with NaCl showed an obvious endothermic peak at about 1173 K (900 °C), which means a drastic reaction between C and CO_2 occurred. However, no obvious endothermic peak was found in the DSC curves of coal without NaCl, from which can be inferred that the gasification reaction was not drastic. The TG-DSC analyses of coal show that NaCl could drastically improve the gasification extent of coal.

2. *Effect of NaCl on reduction*

In order to independently test the influence of NaCl on the reduction of iron oxide in pellets, pellets without coal were reduced by CO to exclude the coal gasification effect in ore–coal composite pellets. Pellets with different NaCl additions were reduced by CO at 1173 K (900 °C) for 35 minutes. The effects of CO flow rate on the reduction of pellets were studied to define changes of reduction results, as presented in Figure 13.

It can be observed that the degree of metallization of reduced pellets increased markedly as the CO flow rose to 4 mL/s. Then the growth gradually tended to be stable as the CO flow rate reached the optimized 10 mL/

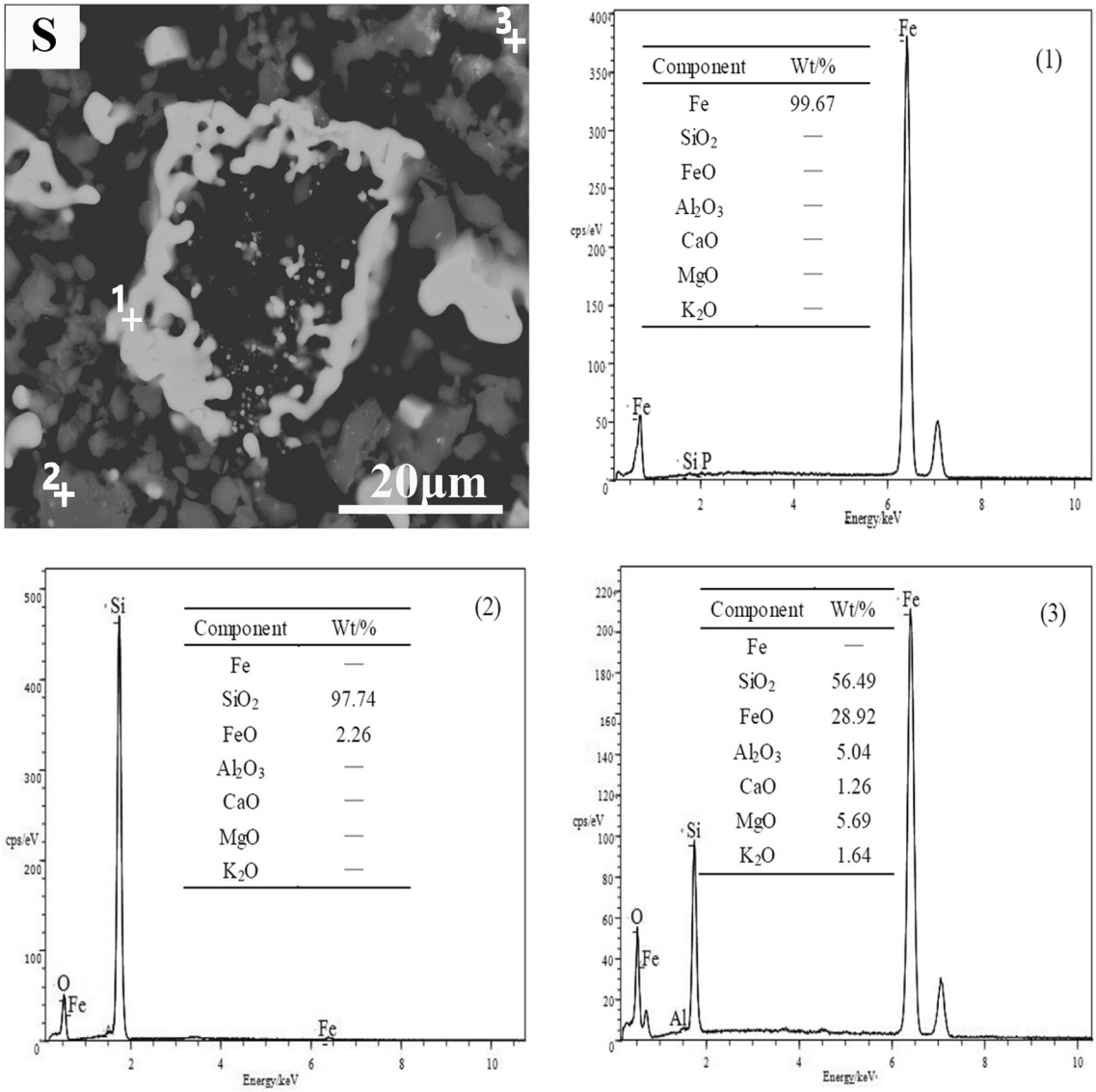

Fig. 17—SEM-EDS analysis of the reduced pellets with 3 mass pct NaCl. S—SEM of reduced pellet. (1), (2), (3)—EDS analyses of positions 1, 2, and 3.

s. However, the difference also apparently existed between pellets with 3 mass pct NaCl and those without.

Pellets with different NaCl additions were reduced by CO at 1173 K (900 °C) for 35 minutes, and the flow rate of CO was 10 mL/s. Figure 14 shows the effect of NaCl on the degree of metallization of reduced pellets. It can be seen that the reduction of iron oxides in pellets was enhanced by NaCl addition. Without NaCl addition, the degree of metallization of 63.25 pct was obtained. However, this value increased to 67.86 pct when the NaCl addition rose to 3 pct. This increase in the degree of metallization can be attributed to the addition of NaCl, which promoted the reaction of FeO to Fe.[31]

C. *Microstructure Characterization of Reduced Composites*

Microstructures of reduced composites (reduced at 1233 K (960 °C) for 55 minutes) were analyzed by SEM-EDS analyses, as shown in Figures 15 through 17, to indicate the difference.

From Figure 15, extremely fine metallic iron particles (bright white) were observed to disperse in pellets without NaCl addition. However, the metallic iron size enlarged obviously with NaCl addition in pellets. Meanwhile, the dispersed iron particles aggregated to a relatively concentrated strip (particularly in Figure 15(d)). This change would greatly facilitate the recovery of iron in the following treatment magnetic separation process. Moreover, the cutback of fayalite phase with NaCl addition was another advantage of the reduction process, which was coincident with the XRD analysis in Section III–A.

As can be seen from Figure 16, the coexisting iron (fine), quartz (platelike), and fayalite (vast) were the main phases in the reduced pellet without NaCl addition. These three showed a close symbiosis. The plentiful fayalite phase hindered not only further reduction of iron oxides but also growth of iron particles. From

Figure 17, iron, quartz, and fayalite still existed in reduced pellets with 3 mass pct NaCl addition. However, their form varied greatly. Instead of dispersed fine particles, iron particles grew into strip shape. All the changes proved the superior reduction and separation characteristics in the sodium addition composite.

IV. CONCLUSIONS

1. The raw ore with characteristics of low iron grade but high SiO_2 content, fine-grained hematite disseminated in gangue substrate was difficult to beneficiate. A low-temperature reduction approach *via* ore–coal composite strengthened by NaCl addition was proposed.
2. The low-grade but high silicon iron ore–coal composite with mol(C/Fe) = 1.4 and 3 pct NaCl addition was reduced at 1223 K (960 °C) for 55 minutes, and a reduced product with degree of metallization of 74.45 pct can be obtained in this study.
3. The gasification process of coal can be greatly facilitated by NaCl addition and, thus, provide sufficient carbon monoxide to the iron oxide reduction. Meanwhile, NaCl can also directly promote the reduction process of iron ore pellets. However, the role seemed weaker than the coal gasification effect.
4. NaCl addition decreased the fayalite formation and enhanced the growth of newly formed iron particles. It was absolutely vital for the low-grade iron ore reduction process.

ACKNOWLEDGMENT

The authors express appreciation to the National Natural Science Foundation of China (Grant No. 51504230) for the financial support of this research.

REFERENCES

1. T.X. Wang, Y.M. Zhu, and X.H. Gui: *J. Cent. South Univ.*, 2016, vol. 23, pp. 1058–65.
2. D.C. Fan, N. Wen, J.Y. Wang, and K. Wang: *J. Wuhan Univ. Technol.*, 2017, vol. 32, pp. 508–16.
3. S. Rachappa, Y. Prakash, and Amit: *Procedia Earth Planet. Sci.*, 2015, vol. 11, pp. 195–97.
4. A.S.S. Ahmed, M.M. Eltahir, and M.A. Abdel-Zaher: *Int. J. Miner. Process.*, 2013, vol. 122, pp. 59–62.
5. B. Das, B.K. Mishra, S. Prakash, S.K. Das, P.S.R. Reddy, and S.I. Angadi: *Int. J. Miner. Metall. Mater.*, 2010, vol. 17, pp. 657–82.
6. X.F. Tang: *Mod. Ming.*, 2014, vol. 3, pp. 14–19 (in Chinese).
7. R.Z. Abd Rashid, S. Mohd, A. Hamzah, H.Y. Mohd, A.A. Nurul, and P.H. Tomohiro: *Renew. Energy*, 2014, vol. 63, pp. 617–23.
8. W. Yu, T.C. Sun, and T.Y. Hu: *ISIJ Int.*, 2015, vol. 55, pp. 329–31.
9. K.Q. Li, W. Ni, and M. Zhu: *J. Iron Steel Res. Int.*, 2011, vol. 11, pp. 9–13.
10. J.Y. Fu, T. Jiang, and D.Q. Zhu: *Sintering and Pelletizing*, Central South University Press, Changsha, 1996, pp. 127–29 (in Chinese).
11. P. Semberg, A. Rutqvist, C. Andersson, and B. Bjorkman: *ISIJ Int.*, 2011, vol. 51, pp. 173–80.
12. A.A. El-Geassy, M.I. Nasr, A.A. Omar, and E.A. Mousa: *ISIJ Int.*, 2008, vol. 48, pp. 1359–67.
13. W.H. Kim, Y.S. Lee, I.K. Suh, and D.J. Min: *ISIJ Int.*, 2012, vol. 52, pp. 1463–71.
14. Y. Man and J.X. Feng: *Powder Technol.*, 2016, vol. 301, pp. 1213–17.
15. D.B. Guo, Y.B. Li, B.H. Cui, Z.H. Chen, S.P. Luo, B. Xiao, H.P. Zhu, and M. Hu: *Chem. Eng. J.*, 2017, vol. 327, pp. 822–30.
16. N.A. El-Hussiny and M.E.H. Shalabi: *Powder Technol.*, 2011, vol. 205, pp. 217–23.
17. Y. Mochizuki, M. Nishio, N. Tsubouchi, and T. Akiyama: *Fuel Process. Technol.*, 2016, vol. 142, pp. 278–95.
18. Q. Wang: *Technology of Composite Pellets*, Metall. Ind., Beijing, 2006, pp. 24–98 (in Chinese).
19. M. Kawanri, A. Matsumoto, R. Ashida, and K. Miura: *ISIJ Int.*, 2011, vol. 51, pp. 1227–33.
20. Z.C. Huang, L.M. Wen, R.H. Zhong, and T. Jiang: *Miner. Metall. Mater. Soc.*, 2016, pp. 461–68.
21. D.Q. Zhu, T.J. Chun, J. Pan, and Z. He: *J. Iron Steel Res. Int.*, 2012, vol. 19, pp. 1–5.
22. G. Wang, Q.G. Xue, and J.S. Wang: *Trans. Nonferrous Met. Soc. Chin.*, 2016, vol. 25, pp. 282–93.
23. S. Coetzee, H.W.J.P. Neomagus, J.R. Bunt, and R.C. Everson: *Fuel Process. Technol.*, 2013, vol. 114, pp. 75–80.
24. Z.W.K. Zhu, W.L. Lin, and W.G. Lin: *Fuel Process. Technol.*, 2008, vol. 89, pp. 890–96.
25. L.L. Zhou and F.H. Zeng: *Adv. Mater. Res.*, 2010, vol. 97, pp. 465–70.
26. S.Z. El-Tawil, I.M. Mosri, and A. Yehiu: *Can. Metall. Q.*, 1996, vol. 35, pp. 31–35.
27. Y. Man, J.X. Feng, Q. Ge, Y.M. Chen, and J.Z. Zhou: *Powder Technol.*, 2014, vol. 256, pp. 361–66.
28. H. Park and V. Sahajwalla: *ISIJ Int.*, 2014, vol. 54, pp. 49–55.
29. K. Sinha, T. Sharma, and D.D. Haladar: *Int. Eng. Adv. Technol.*, 2014, vol. 3, pp. 30–33.
30. N.S. Srinivasan and A.K. Lahiri: *Metall. Trans. B*, 1977, vol. 8B, pp. 175–78.
31. D.S. Chen, B. Song, L.N. Wang, T. Qi, Y. Wang, and W.J. Wang: *Miner. Eng.*, 2011, vol. 24, pp. 864–69.